Evaluating and predicting fatigue behavior in adhesively bonded joints

Ashcroft, Ian; Pascoe, John Alan

DOI
10.1016/B978-0-323-91214-3.00026-0

Publication date
2023

Document Version
Final published version

Published in
Advances in Structural Adhesive Bonding, Second Edition

Evaluating and predicting fatigue behavior in adhesively bonded joints

19

Ian Ashcroft[a] *and John-Alan Pascoe*[b]
[a]University of Nottingham, Nottingham, United Kingdom, [b]Delft University of Technology, Delft, The Netherlands

19.1 Introduction

Like most other engineering materials, adhesives suffer from fatigue, that is, the degradation of material properties and eventual failure due to repeated load cycles below the static strength of the material. Evaluating the fatigue life of an adhesive joint is therefore crucial to ensuring the durability of an adhesively bonded structure. Besides looking purely at research on adhesive bonds, we can also draw lessons from research on delamination of composites, which often involves similar materials (e.g., epoxy systems) in similar geometries (cracking of a thin layer between two stiffer adherends).

Over the years, a number of different approaches have been developed for evaluating the fatigue life of adhesive bonds. These can be grouped into four categories:

1. **Stress/strain-life approaches** that link the applied stress or strain amplitude to the fatigue life of the joint, without further consideration of the physical damage processes.
2. **Strength/stiffness wearout models** in which the strength and/or stiffness of the joint is gradually reduced as a function of the number of applied load cycles. Final failure occurs when the strength or stiffness reaches a critical value.
3. **Fracture mechanics models** that model the growth of the physical crack(s) in the adhesive joint. Final failure occurs when the crack reaches a critical size.
4. **Damage mechanics** that represent the damage in the material by a damage parameter, which usually can range from 0 (undamaged) to 1 (fully damaged), and in which damage will progressively increase as a function of fatigue cycles until failure occurs. Damage mechanics approaches are usually implemented within finite element analyses.

This chapter will first cover some general considerations in evaluating fatigue in adhesive joints and then discuss the available experimental techniques. Next, a more in-depth discussion will be presented on the four categories of prediction models mentioned above. Finally, the influence of various features of the joint (e.g., adhesive thickness and joint geometry) and the influence of environmental effects on the fatigue life will be discussed.

Advances in Structural Adhesive Bonding. https://doi.org/10.1016/B978-0-323-91214-3.00026-0

19.2 General considerations for fatigue of adhesives

The fatigue behavior of an adhesive bond will depend on many factors. These include the amplitude and frequency of the applied load cycles, the environmental conditions, the adherend and adhesive materials and geometry, and the surface treatment applied before the bonding process. These factors do not just influence the rate at which specific fatigue mechanisms propagate, but can also change which fatigue mechanisms occur in the first place.

Adhesively bonded joints are multimaterial structures and therefore can suffer from different failure modes, as illustrated in Fig. 19.1. Bonded joints can fail through cohesive failures of either the adherends (Fig. 19.1a) or the adhesive (Fig. 19.1b). In metals, cohesive adherend failure typically takes the form of a transverse crack through the thickness of the adherend, initiated at a stress concentration near the end of the bond line (Fig. 19.1a). In fiber-reinforced composites, on the other hand, if the interlaminar interface is weaker than the adhesive, delamination of the ply or plies closest to the adhesive may occur (Fig. 19.1a). Cohesive failure of the constituent materials of the joint failure can also occur due to a failure of the adhesion between the adhesive and one of the adherends (Fig. 19.1c). It is also possible for a joint to fail through a combination of cohesive failure in both the adhesive and the adherend (Fig. 19.1d) or by a mix of both cohesive and interfacial failure. In the case of metal adherends, the stress concentration generated by the presence of a crack in the adhesive can initiate a crack in the adherend as well. In the case of composite adherends, the crack can migrate into the composite and continue growing as a delamination. In some cases, the crack can even migrate back to the bondline at a later stage, for example in the scarf joints investigated by Goh et al. [1]. The propensity of the crack to migrate depends on the joint geometry and the lay-up of the adherends [2]. In general, a crack will find it more difficult to migrate through a layer where the fibers are aligned parallel to the (local) loading direction, and easier to migrate through a layer where the fibers are aligned perpendicular to the loading direction. This is because in the second case, the crack can propagate through the layer as a purely matrix crack, without needing to break any fibers.

When trying to predict or analyze the fatigue behavior of a specific structure in service, it's important to ensure that any analyses or experiments used to support this are based on the same failure mode. If the failure mode seen in service does not match that seen in the lab, or assumed in the analysis, then that analysis result or experimental data are not applicable to the case under examination.

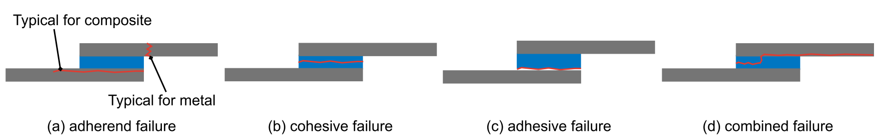

Fig. 19.1 The different failure modes that can occur in an adhesive bond.

19.3 Experimental techniques

Experimental data are essential for evaluating the fatigue performance of adhesive bonds. Although various fatigue models exist, they all require experimental data on the fatigue behavior of some kind, and thus specific fatigue experiments are needed. Tests can be performed for different reasons, such as part of material screening and selection, to provide input for predictive models or to validate fatigue analyses. In the case of tests performed to provide input for predictive models, the type of model will determine the test objectives. For stress or strain-life approaches, the objective is to determine the number of cycles until failure at different load levels and thus only the applied load needs to be determined accurately. To support damage mechanics or wearout models, the objective is to obtain the residual strength or stiffness as a function of the number of cycles. Measurement of the residual stiffness requires some consideration to ensure a sufficiently accurate measurement can be obtained. To support fracture mechanics models, tests need to determine the fracture mechanics parameters and accurately measure the crack growth rate. Thus, specimens need to be selected in which the crack length can be readily measured. For experiments aiming to detect fatigue crack initiation, configurations can be selected where initiation can be detected through strain measurements, such as Refs. [3–8].

Typically, the test specimen geometries used for fatigue testing are similar to those used for quasistatic testing, but with a cyclic load applied instead of a monotonic one. Some commonly used fatigue test geometries are shown in Fig. 19.2. Besides the coverage in this chapter, some test methods are also discussed in more detail in Chapters 14, 16, 17, 20–22, and 32. Testing aimed at finding the fatigue life commonly makes use of lap joints, which are covered by the BS EN ISO 9664:1995 and ASTM D3166-99 standards. For the crack growth parameters needed for fracture mechanics models, test geometries such as the double cantilever beam (DCB, mode I, Fig. 19.2d), end notch flexure (ENF, mode II, Fig. 19.2e), or mixed-mode bending (MMB, mixed-mode, Fig. 19.2f) can be employed. As of yet, no test standards have been published for fatigue crack growth tests, but for double cantilever beam tests, the quasistatic standards ASTM D3433-99 or ISO 25217 can be used as a basis for the specimen

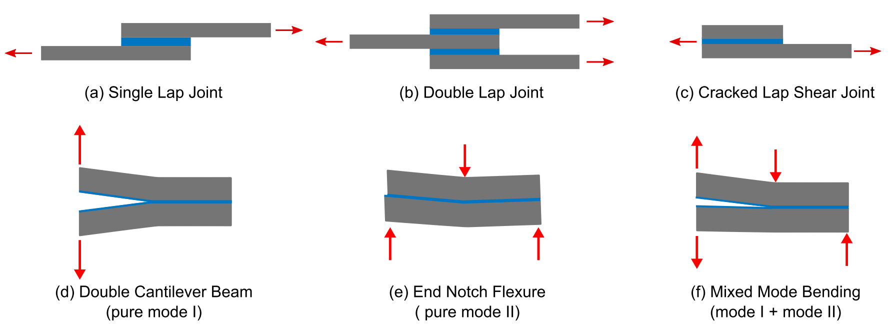

Fig. 19.2 Examples of commonly used fatigue test geometries.

geometry. It is important to note that the standard fracture mechanics tests assume that the crack occurs at the midplane between two arms made of the same material. Therefore, special care needs to be taken when investigating the bonding of two dissimilar materials (e.g., metal to fiber-reinforced polymer). A typical approach is to adjust the thickness of each arm so that the bending stiffness is equal [9–12], although in that case the strains at the interface might still be quite different, resulting in different behavior, even if the global strain energy release rate appears to be the same.

If the goal of a test is to measure the crack propagation rate, a longer overlap length than employed for quasistatic tests may be desirable to avoid premature failure of the specimen. For testing the behavior of long bond lines, such as those of bonded stiffeners, the cracked lap shear (CLS) configuration (Fig. 19.2c) is a popular choice. This configuration can reproduce the stress concentration caused by a stiffener run-out and can therefore be used to investigate the fatigue initiation behavior. It also reproduces the change of mode-mixity as the crack grows. Lai et al. [13] have provided a closed-form solution for this configuration.

An extensive review of available testing methods for adhesive bonds has recently been provided by Budzik et al. [14]. They point out that there are only a limited number of generic test standards (this is even more the case for fatigue) and that in practice, much testing is conducted using industry- and/or application-specific methods. This situation is likely in part due to the difficulty of generalizing experimental results. The stress distribution in an adhesive joint is complex and highly dependent on both the joint geometry and the adherend properties. Furthermore, if a geometry is used in which multiple cracks may occur (e.g., a double strap joint), these cracks can interact with each other [15]. Therefore, it can be difficult to transfer results obtained in a certain experiment to predict the behavior of a joint with a different geometry, even if the same adhesive and adherends are used. Additionally, it should be kept in mind that the adherend properties will influence the test results. Thus, without extensive analysis, a test will give information on the combination of adherend and adhesive under the specific joint configuration and loading mode, rather than on the material properties of the adhesive itself. As a recent example, Sahin and Alkpinar [16] investigated the effect of adherend thickness on the fatigue strength of bonded single-lap joints. They found that an increase of the adherend thickness resulted in an increased fatigue strength in terms of the applied force, but by a much smaller factor than the increase in adherend thickness. For example, increasing the adherend thickness from 2 to 5 mm increased the fatigue strength by only 24% due to the change in bending moments and flexural stiffnesses of the adherends. Thus, a change in adherend thickness needs to be accounted for when comparing two different cases.

When conducting tests to predict the behavior of an operational structure, particular attention should be paid to using the same manufacturing process for both test specimens and the final structure, as changes in the manufacturing procedure will affect the fatigue life [17]. An illustrative case study here is the wing root joint of the F/A-18 fighter jet, also discussed in Chapter 23. This is a stepped-lap joint in which a titanium lug is adhesively bonded to a composite skin, as shown in Fig. 19.3. In order

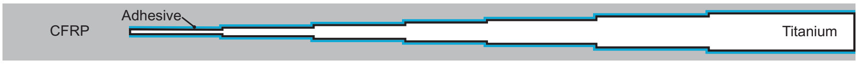

Fig. 19.3 The F/A-18 wing root joint.

to investigate possible safety concerns, and to support a life extension program, Seneviratne et al. tested the residual strength and remaining fatigue life of specimens cut from retired aircraft wings that had been used in service [18]. These tests showed that the remaining strength and fatigue life were satisfactory, and the specimens failed through cohesive failure in either the adhesive or adherend (as required) in all cases. Nevertheless, at a later stage large disbonds were discovered on a number of aircraft in service, and these were investigated by Mueller et al. [19]. The investigation found that the disbonds took the form of *adhesive* failure, rather than the cohesive failure that occurred in the Seneviratne et al. test program. After further investigation, it was concluded that the most likely cause was a failure to sufficiently rinse off fluorine-containing residue during the surface treatment. Effectively, the insufficient rinsing in the specimens examined by Mueller et al. meant that they had undergone a slightly different manufacturing process than the specimens used by Seneviratne et al., which were taken from a different aircraft than the failures examined by Mueller et al. This resulted in a change of failure modes when the joints were subjected to fatigue loading, which meant that the results obtained by Seneviratne et al. were not applicable, even though they were obtained from nominally identical joints. These results highlight the potential impact of surface treatment and manufacturing processes, and imperfections in those processes, on the behavior of the joint. For further discussion of surface issues, see Chapter 9. As a general lesson, this case study shows the importance of carefully evaluating under which conditions experimental results can actually be applied to operational structures.

19.4 Stress/strain-life approaches

19.4.1 The stress-life approach

This constitutes one of the earliest approaches to predicting fatigue, as pioneered by Wöhler [20] in his studies of failure in iron and steel in the railways. It is an empirical approach based on testing samples under constant sinusoidal loading at various load levels. The number of cycles to failure (N_f) is then plotted as a function of a variable such as stress or strain amplitude. Where the loading is low enough that the deformation is predominantly elastic, a stress variable (S) is usually chosen and the resultant plot is termed an S-N curve, or a Wöhler plot; this is known as the stress-life approach. Under these conditions, a long fatigue life would be expected and hence this is sometimes termed high cycle fatigue (HCF). The S-N data are either plotted as a log-linear or a log-log plot and a characteristic equation can be obtained by empirical curve fitting. The constants in the curve-fitted equations are dependent on many factors, including material, geometry, surface condition, environment, and mean stress. Hence, caution should be used when trying to apply *S-N* data beyond the samples used to generate the data. The standard stress-life method gives no indication of the progression of damage, although in some cases the onset of cracking is indicated on the plot in addition to the complete failure, hence allowing the initiation and propagation phases to be differentiated. The above factors mean that the *S-N* curve is of rather limited use in predicting fatigue behavior; however, it is still useful in fatigue modeling as a validation tool, such as with [21,22].

A further limit in the application of *S-N* curves to fatigue prediction in bonded joints is that there is no unique relation between the easily determined average shear stress in the adhesive layer and the maximum stress. For this reason, load rather than stress is often used in total-life plots for bonded joints; these are known as *L-N* curves. A typical *L-N* curve for epoxy-bonded double-lap joints can be seen in Fig. 19.4. The *L-N* curve can be divided into a low cycle fatigue (LCF) region below approximately 1000 cycles, a high cycle fatigue (HCF) region between approximately 1000 and 100,000 cycles, and an endurance limit region, which in this case starts at approximately 100,000 cycles. The endurance limit is defined by a load below which an infinite fatigue life is predicted. However, not all materials exhibit a clearly defined endurance limit, in which case it may be instead defined as the load at which fatigue failure hasn't occurred after a large number of cycles representative of the application, typically 10^6.

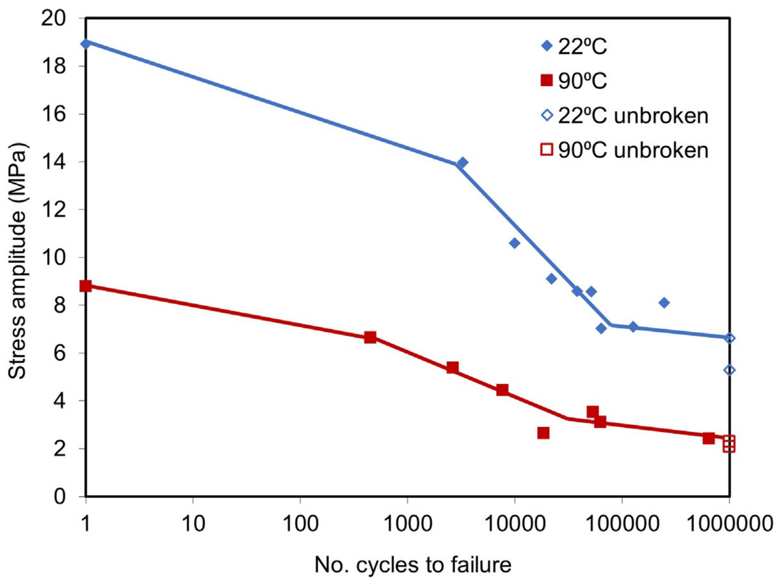

Fig. 19.4 Load-life (*L-N*) curve for bonded lap joints.
Data from I.A. Ashcroft, D.J. Hughes, S.J. Shaw, M.A. Wahab, A. Crocombe, Effect of temperature on the quasi-static strength and fatigue resistance of bonded composite double lap joints, J. Adhes. 75(1) (2001) 61–88.

Fatigue life not only depends on the stress amplitude but also on the mean stress, as either increasing the mean or increasing the amplitude tends to result in a reduction of the fatigue life. The relationship between amplitude and mean on the fatigue life can be illustrated in constant-life diagrams, in which a given fatigue life is plotted against both mean and amplitude.

19.4.2 Damage initiation and crack growth phases of damage

Although the *S-N* curve can be used to predict life to failure for a particular load or stress that sits on the experimental plot, it tells us nothing of the evolution of damage in a component. A particular deficiency in the standard stress-life approach is that no differentiation is made between the crack initiation and growth phases. In some cases, efforts have been made to differentiate between the initiation and propagation phases in the *S-N* behavior of bonded joints [4,23–28]. Shenoy et al. [26] used a combination of back-face strain measurements and sectioning of partially fatigued joints to measure damage and crack growth as a function of number of fatigue cycles. It was seen from the sectioned joints that there could be extensive internal damage in the joint without external signs of cracking; therefore, the determination of an initiation phase from external observations alone is likely to lead to an overestimation. Shenoy et al. [26] identified three regions in the fatigue life of an aluminum/epoxy single-lap joint: an initiation period (CI) in which damage starts to accumulate, but a macrocrack has not yet formed; a stable crack growth (SCG) region in which a macrocrack has formed and is growing slowly; and a fast crack growth region (FCG), which leads to rapid failure of the joint. They found that the percentage of life spent in each region varies with the fatigue load. At low loads, the fatigue life is dominated by crack initiation, whereas crack growth dominates at high loads. This is illustrated schematically in the extended *L-N* curve of Fig. 19.5. It can also be seen in the figure that the back-face strain signal associated with each phase of fatigue damage can be used to monitor damage.

19.4.3 Variable amplitude fatigue

The *S-N* curve is only directly applicable to constant amplitude fatigue, whereas in most practical applications for structural joints, a variable amplitude fatigue spectrum is more likely. A simple method of using *S-N* data to predict variable amplitude fatigue is that proposed by Palmgren [29] and further developed by Miner [30]. The Palmgren Miner (P-M) rule can be represented by:

$$\sum \frac{n_i}{N_{fi}} = 1 \qquad (19.1)$$

where n_i is the number of cycles in a constant amplitude block, and N_{fi} is the number of cycles to failure at the stress amplitude for that particular block and can be obtained from the *S-N* curve. It can be seen by using Eq. (19.1) that the fatigue life of a sample in variable amplitude fatigue can be predicted from an *S-N* curve obtained from

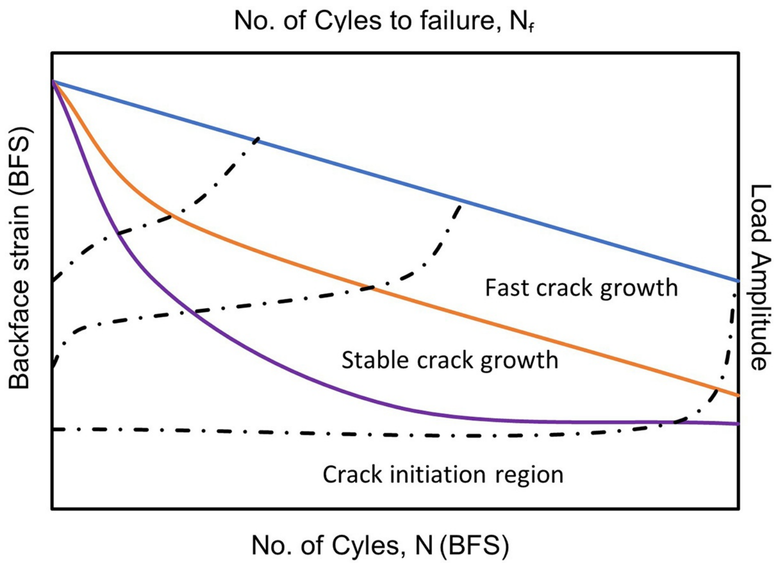

Fig. 19.5 Extended *L-N* diagram.
From V. Shenoy, I.A. Ashcroft, G.W. Critchlow, A.D. Crocombe, M.M. Abdel Wahab, An investigation into the crack initiation and propagation behaviour of bonded single-lap joints using backface strain, Int. J. Adhes. Adhes. 29(4) (2009) 361–371.

constant amplitude fatigue testing of similar samples. However, there are a number of serious limitations to this method, primarily the assumptions that damage accumulation is linear and that there are no load history effects. Modifications to the P-M rule have been suggested to address some of the deficiencies, such as with [31–35]. However, any improvements are at the expense of increased complexity and/or increased testing requirements and the basic flaw in the method, that it bears no relation to the actual progression of damage in the sample, is still not addressed. Erpolat et al. [36] used the P-M law and the extended P-M law, in which cycles below the endurance limit also contribute to damage accumulation, to predict failure in an epoxy-CFRP double lap joint subjected to a variable amplitude (VA) fatigue spectrum. The resulting Miner's sum was significantly less than 1, varying between 0.04 and 0.3, and decreased with increasing load. This indicates that load sequencing is causing damage acceleration, that is, that the P-M rule is nonconservative.

19.4.4 Fatigue limit

Wöhler [20] noted a stress below which a nominally infinite life is seen, which is termed the fatigue or endurance limit. If a fatigue limit is seen, then it may be possible to use the data from one sample to predict the fatigue limit for a different geometry or loading condition. The approach is similar to that for predicting failure under quasistatic loading, and similar multiaxial failure criteria, such as von Mises or maximum principal stress, should be used. Wahab et al. [37] compared the predicted fatigue limit (or fatigue threshold) in bonded lap-strap joints using a variety of stress- and strain-based failure criteria. It should be noted that many materials do not have a well-defined fatigue limit, in which case a high number of cycles such as 10^7 may be used to indicate a nominal fatigue limit for predictive purposes.

19.4.5 The strain-life approach

Under high stress amplitudes, plastic deformation occurs and the fatigue life is considerably shortened. This is known as low cycle fatigue (LCF). Under constant stress amplitude fatigue with strain hardening, the strain amplitude decreases after the first cycle, and the subsequent hysteresis loop is repeated a number of times before microcracking occurs. In LCF, the high loads and plastic deformation mean that the fatigue life is dominated by crack initiation as failure occurs quickly once a crack has formed. This behavior can be seen in Fig. 19.5 and also explains the change in gradient of the *L-N* curve in Fig. 19.4 in the LCF region. In constant strain amplitude testing, if there is a positive strain mean then the mean tends to decrease as the sample is fatigued, a phenomenon known as plastic shakedown. This can be compared with the effect of creep in constant stress amplitude testing, which leads to an increase in the mean strain with cycling. The strain-life approach is more difficult to implement than the stress-life method, particularly for complex systems such as bonded joints. Structural bonded joints tend to be used in HCF applications and hence the strain-life method has seen little application to adhesively bonded joints.

19.5 Strength/stiffness wearout

An alternative phenomenological approach to the total life methods described above is to characterize fatigue damage as a function of the reduction in the strength or stiffness of the joint during its fatigue life. Stiffness wearout has the advantage that it can be detected by nondestructive testing techniques; however, it is not directly linked to a failure criterion and may not be very sensitive to the early stages of damage. The strength wearout method provides a useful characterization of the degradation of residual strength with fatigue cycling but requires extensive destructive testing.

19.5.1 Strength wearout approach

In the strength wearout method, the joint's strength is initially equal to the static strength, S_u, but decreases to $S_R(n)$ as damage accumulates through the application of n fatigue cycles. This degradation can be represented by:

$$S_R(n) = S_u - f(S_u, S_{\max}, R)n^k \tag{19.2}$$

where κ is a strength degradation parameter, $S_{\max}$ is the maximum stress, and R is the ratio of minimum to maximum stress (i.e., $R = S_{\min}/S_{\max}$). Failure occurs when the residual strength equals the maximum stress of the spectrum, that is, when $S_R(N_f) = S_{\max}$.

Shenoy et al. [38] proposed a modified version of this equation that they termed the normalized nonlinear strength wearout model (NNLSWM), which is given by:

$$L_n = 1 - \frac{(L_u - L_{\max})}{L_u}(N_n)^{\eta} \tag{19.3}$$

The normalized residual failure load, L_n, and normalized cycles to failure, N_n, are defined as:

$$L_n = {}^{L_R(n)}\!/\!{}_{L_u}$$
$$N_n = n/N_f$$

where $L_R(n)$ is the quasistatic failure load after n fatigue cycles, L_u is the quasistatic failure load prior to fatigue loading, and N_f is the number of cycles to failure. Fig. 19.6 shows an experimental plot of L_n against N_n for various fatigue loads, together with the best fit of Eq. (19.3). It can be seen that the proposed phenomenological model agrees well with the experimental results. A single curve can be reasonably drawn for the entire range of fatigue loads, wherein the experimental parameter η is independent of the applied fatigue load.

Schaff and Davidson [40,41] extended Eq. (19.2) to enable the residual strength degradation of a sample subjected to a variable amplitude loading spectrum to be predicted. However, they noted a crack acceleration effect in the transition from one constant amplitude (CA) block to another, a phenomenon they termed the cycle mix effect, and proposed a cycle mix factor, CM, to account for this. Erpolat et al. [42] proposed a modified form of Shaff and Davidson's cycle mix equation to model the degradation of CFRP-epoxy double-lap joints subjected to a variable amplitude

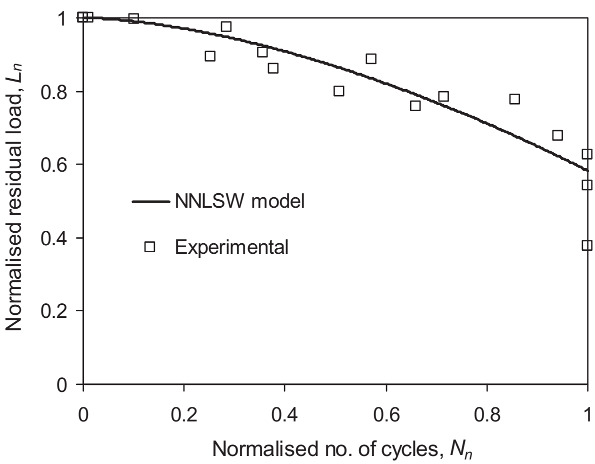

Fig. 19.6 Normalized nonlinear strength wearout model (Shenoy et al. [39]).

fatigue spectrum. They showed that this model represented the fatigue life of bonded joints under variable amplitude fatigue more accurately than Palmgren-Miner's law. Shenoy et al. [39] proposed further modifications to this approach based upon a nonlinear strength wearout model with a damage-dependent cycle mix parameter. It is worth noting that whereas crack acceleration is seen after overloads in brittle thermosetting plastics, such as epoxies, the opposite is frequently reported for ductile metals, where plastic deformation can cause crack blunting, strain hardening, and/or plasticity-induced crack closure [43]. It could be postulated, therefore, that in more ductile adhesives in which failure is dominated by plastic yielding rather than crack growth, overloads may be less detrimental or even beneficial in terms of fatigue life.

19.5.2 Stiffness wearout approach

As with strength degradation, the stiffness degradation rate can be considered a power function of the number of load cycles, using a similar equation to 2 [44–46]. A failure criterion for a stiffness-based wearout model is not as straightforward as that for the strength-based wearout models. One approach is to relate the degraded stiffness, $E(N_f)$, to stress, such as:

$$\frac{E(N_f)}{E(0)} = \frac{S_{\max}}{S_u} \tag{19.4}$$

where $E(0)$ is the initial stiffness.

19.6 Fracture mechanics

The fracture mechanics-based approaches to fatigue aim to predict the growth of physical cracks in the adhesive bond. The fatigue life of the bond is reached when the crack reaches a critical length. This is usually defined as the crack length at which unstable fracture occurs if the maximum design load is applied. An important advantage of these kinds of approaches is that they can be used to analyze the effect of defects on the fatigue life [47], unlike stress/strain-life approaches, which are usually based on (nominally) "defect-free" specimens.

Typically, researchers aim to predict the crack growth rate based on linear elastic fracture mechanics (LEFM) theory (see also Chapters 15–17 and 32). LEFM was first applied to the prediction of fatigue crack growth in metals by Paris and coworkers [48]. Some 15 years later, Mostovoy and Ripling [49] adopted this approach for fatigue crack growth in adhesives. For this, Mostovoy and Ripling modified the equation proposed by Paris by replacing the stress intensity factor range ΔK with the strain energy release rate range (SERR) ΔG to obtain an equation of the form:

$$\frac{da}{dN} = Cf(G)^n \tag{19.5}$$

where da/dN is the crack growth rate, C and n are empirical parameters found by curve fitting, and $f(G)$ is a function of the strain energy release rate. It should be noted that ΔG is proportional to $(K_{max}^2 - K_{min}^2)$, which is not equal to $\Delta K^2 = (K_{max} - K_{min})^2$. Therefore the substitution of ΔG for ΔK is not directly equivalent in a physical sense [50]. Nevertheless, Mostovoy and Ripling were able to successfully correlate the crack growth rate to ΔG. As an alternative to ΔG, other researchers have suggested $f(G) = G_{max}$ or $f(G) = \Delta\sqrt{G} = \sqrt{G_{max}} - \sqrt{G_{min}}$. As long as the empirical parameters C and n are calibrated to match the choice of $f(G)$, all three choices can result in good fits of experimental crack growth data. Many variations on the basic form of Eq. (19.5) have been proposed over the years, for example to deal with the R-ratio or mode-mixity effects, and reviews can be found in Refs. [51–53].

LEFM assumes a linear elastic material behavior and is therefore usually only applied for brittle adhesives such as epoxies (including toughened epoxy systems). In cases where the adhesive exhibits significant amounts of plasticity during fatigue loading, the SERR may not be the most appropriate controlling parameter. In these cases, the J-integral (discussed in detail in Chapter 16) may prove to be a suitable alternative to the SERR. Several researchers have therefore proposed fatigue and/or crack growth models based on the J-integral as the controlling parameter [37,54–56], but there does not yet seem to be widespread adoption of this approach. For both the J-integral and LEFM approaches, the key issue is how to relate the chosen driving force representation (e.g., J_{max} or ΔJ) to the crack growth rate. To date, no physical theory has been formulated that can justify the form of Eq. (19.5), and thus, fracture mechanics approaches rely on empirical correlations. Nevertheless, given sufficient input data, these methods can still produce accurate predictions. Care does need to be taken to ensure that the input data match the prediction case, as for example R--ratio, mode-mix, and environmental effects are known to affect the values of the fitting parameters C and n. Also, other factors such as manufacturing quality and loading frequency may also affect the crack growth behavior.

19.6.1 Numerical techniques

For simple geometries, analytical equations are available to calculate the strain energy release rate, as for example provided in the ASTM D5528-13 (DCB), ASTM D6671M-19 (MMB), and ASTM D7905M-14 (ENF) standards. The crack length after a certain number of cycles can then be predicted by inserting the strain energy release rate equation into Eq. (19.5) and integrating. For more complex geometries, however, simple equations for the strain energy release rate are not available, and thus finite element analysis (FEA) is called for. With FEA, one popular method for calculating the strain energy release rate is the virtual crack closure technique (VCCT), originally developed by Rybicki and Kanninen [57], based on an argument by Irwin [58]. The basic assumption is that the energy released when extending the crack by a certain increment is the same as the work required to close the crack by the same increment. Thus, the strain energy release rate at a certain node in a finite element mesh can be computed based on the nodal forces, and the displacements of the nodes behind the crack tip. An overview of earlier development and applications of VCCT has been provided by Krueger [59]. More recently, guidelines for implementing VCCT-based fatigue analyses have been published by NASA [60]. Because the VCCT allows calculation of the strain energy release rate within the numerical analysis, it can be combined with Eq. (19.5) to predict the crack growth rate. The VCCT has downsides, however, including that remeshing is required when a crack grows and that an initial crack is always required. Also, the VCCT cannot model crack initiation.

To improve on the limitations of VCCT, recent research efforts have focused on the use of cohesive zone models (CZM) to predict fatigue crack growth, such as [61–72]. The cohesive zone models are based on the works of Dugdale [73] and Barenblatt [74], and were applied to the fatigue of adhesive bonds by Pirondi and Moroni [75,76]. While the details of implementations differ, the CZMs are all based on a constitutive law linking traction to the separation of nodes. As separation is increased, the traction first increases until a critical separation is reached, after which it decreases, thereby simulating the initiation of damage. The irreversible nature of the damage is simulated by introducing one or more damage parameters, which are used to degrade the stiffness of the element. Fatigue damage can be simulated by incrementing the damage parameters based on the loading and the number of cycles that have been applied. Rather than simulating the effect of each individual cycle, which would be computationally very costly, a cycle jump strategy is usually applied in which the crack growth rate is effectively assumed to remain constant for a certain increment of cycles. The increment of the damage parameters due to fatigue is usually chosen such that it will produce the crack growth rate predicted by Eq. (19.5). Therefore, although one can argue that the cohesive model is more representative of the actual material behavior, it is important to realize that when it comes to representing fatigue behavior, cohesive zone-based models still rely on an empirical correlation to predict the crack growth.

19.6.2 R-*ratio effect*

Many researchers have noted that the ratio of minimum to maximum stress in a cycle, the R-ratio-affects the crack growth rate. That is, if $G_{\max}$ or ΔG is held constant and the R-ratio is changed, then a different crack growth rate is obtained. This should not be very surprising, as the combinations of a particular $G_{\max}$ or ΔG value and two different R-ratios specify two different load cycles, which then also produce two different crack growth rates. The qualitative effect of changing the R-ratio can be predicted by considering the amount of cyclic work, U_{cyc}, that would be applied. For example, if the amount of cyclic work is reduced (e.g., by keeping $G_{\max}$ constant and increasing R), then the crack growth rate will be lower [77]. The effect of R-ratio on cyclic work when holding different LEFM parameters constant is illustrated in Figs. 19.7 and 19.8.

If ΔG is held constant and the R-ratio is changed, then U_{cyc} remains constant. Thus, one might expect the crack growth rate to also remain constant. This is indeed sometimes seen [77]. However, in other cases, increasing the R-ratio while keeping ΔG constant results in a reduction in the crack growth rate [50,78]. The likely reason for this is that keeping ΔG constant while increasing R also requires increasing $G_{\max}$. In Ref. [77], which investigated an epoxy adhesive, increasing $G_{\max}$ was correlated to

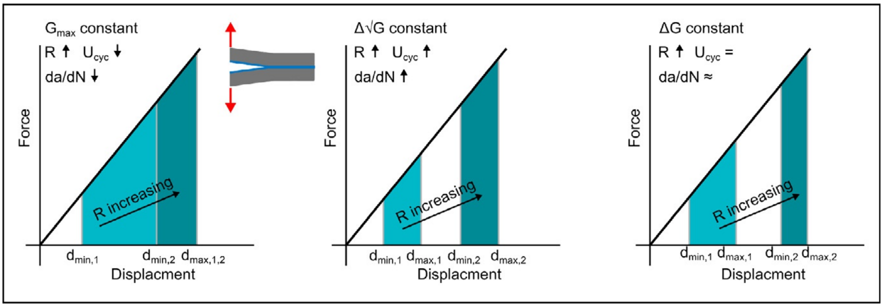

Fig. 19.7 Effect of changing R-ratio on cyclic work (U_{cyc}) and crack growth rate (da/dN) while hodling different LEFM parameters constant.

an increase of the resistance to crack growth, that is, the amount of energy required to advance the crack by a unit distance, which results in a reduction of the crack growth rate. The previous discussion is mainly based on data from epoxy adhesives and matrices, though a similar effect of R-ratio on the Paris curve has been reported for a thermoplastic PEEK-based composite [79]. Interestingly, Jia and Davalos [80] reported a different behavior for the case of a resorcinol-formaldehyde adhesive used to bond wood to a fiber-reinforced polymer. There, an increasing da/dN for a constant ΔG resulted in an increased crack growth rate. Further research is still needed to understand the physics of this R-ratio effect.

This lack of understanding means that there is as yet no theoretical model that can a priori quantitatively predict the R-ratio effect on the crack growth rate. Instead, an empirical model is needed that can account for the R-ratio. The most basic approach is to experimentally determine the values of the coefficient and exponent in Eq. (19.5) for different R-ratios. This will require a substantial experimental effort, and is therefore undesirable. Instead, the basic form of Eq. (19.5) can be modified to either explicitly include the R-ratio as an input variable, or to describe the load cycle by two parameters. Various options have been presented in the literature, mainly based on data from epoxy systems. One possibility is the use of the Hartman-Schijve equation, as proposed by Jones and Kinloch [81,82]:

$$\frac{da}{dN} = D(\Delta\kappa)^n = D\left[\frac{\Delta\sqrt{G} - \Delta\sqrt{G_{\mathrm{thr}}}}{\sqrt{1 - \sqrt{G_{\max}/A)}}}\right]^n \tag{19.6}$$

where $\Delta\sqrt{G_{\mathrm{thr}}}$ is the value of $\Delta\sqrt{G}$ at the threshold below which no significant fatigue crack growth occurs and A is the critical value of $G_{\max}$, at which the crack growth rate asymptotically goes to infinity. A is therefore close to the quasistatic fracture toughness G_c, but not necessarily equal to it. Because this expression uses two parameters to specify the fatigue cycle (i.e., $G_{\max}$ and $\Delta\sqrt{G}$), it can uniquely define the cycle. In addition to this, Jones and Kinloch suggest accounting for the R-ratio by varying the value of $\Delta\sqrt{G_{\mathrm{thr}}}$ [81]. Similarly, adjusting the value of $\Delta\sqrt{G_{\mathrm{thr}}}$ and A,

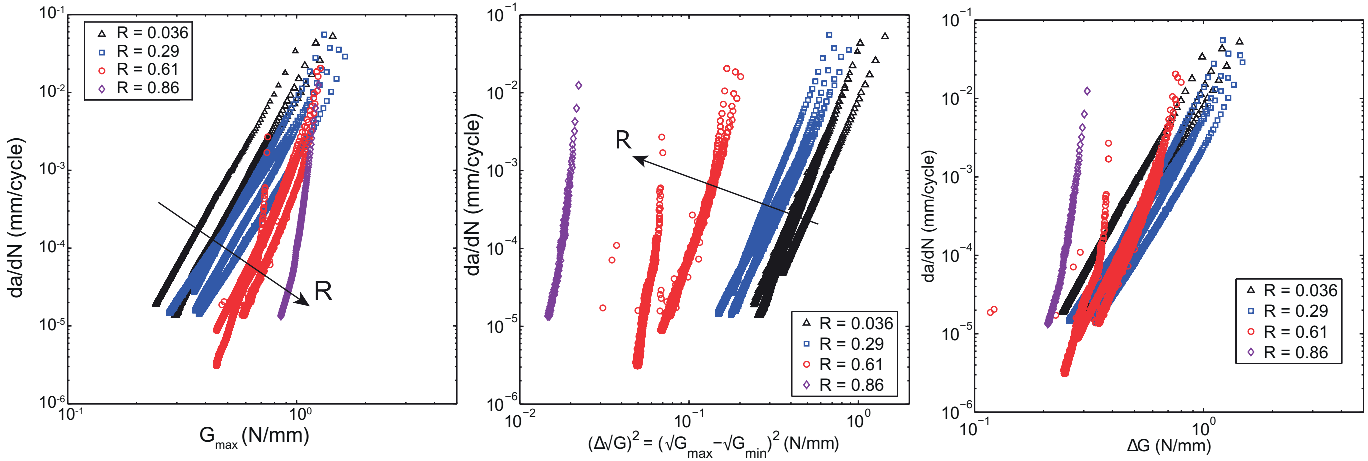

Fig. 19.8 Effect of different *R*-ratios depending on the chosen LEFM similitude parameter. Data showing crack growth in an epoxy adhesive from [77].

based on experimental data, can capture the effect of temperature, mode mix, and adhesive thickness and collapse the data onto a single master curve [82]. The other two parameter models are those of Khan [83]:

$$\frac{da}{dN} = C_1 G_{\max}^{n_1} + C_2 \Delta G^{n_2} \tag{19.7}$$

and Atodaria et al. [84]:

$$\frac{da}{dN} = C\left[\left(\sqrt{G}\right)_{\text{average}}^{\gamma}\left(\Delta\sqrt{G}\right)^{1-\gamma}\right]^{n} \tag{19.8}$$

$$\sqrt{G_{\text{average}}} = \left[\frac{1}{k}\sum_{\sqrt{G_{\text{thr}}}}^{\sqrt{G_{\max}}}\left(\sqrt{G}\right)^{w}\right]^{\frac{1}{w}} \tag{19.9}$$

where the range from $\sqrt{G_{\text{thr}}}$ to $\sqrt{G_{\max}}$ is divided into k increments, w is an experimentally determined weight factor, and γ is an empirical mean stress sensitivity parameter. Instead of using two parameters to describe the load cycle, one can instead explicitly include the R-ratio in the equation, as in the model of Allegri et al. [85]:

$$\frac{da}{dN} = C\left(\frac{G_{II,\max}}{G_{IIc}}\right)^{\frac{n}{(1-R)^2}} \tag{19.10}$$

Eq. (19.10) is formulated in terms of the mode II SERR, but of course a similar formulation could be made for mode I crack growth. The models mentioned above only give limited insight into the physical mechanisms underlying the fatigue crack growth process. Nevertheless, as an engineering approach they can provide accurate crack growth rate predictions under different R-ratios, if suitable experimental data are available.

19.6.3 Mode mix

In structural applications, bonded joints will often be subjected to mixed-mode loading (also discussed in Chapters 17 and 32), and the mode-mixity can vary along the crack front. In some cases, especially if there is tension-compression fatigue inducing buckling in the adherends, the mode-mix could even change depending on the phase of the load cycle. Therefore, understanding the effect of mode-mixity on crack growth rate and/or fatigue life is an area of active research [63,72,86–92].

In general, it can be stated that crack growth under mode I loading for a given applied G-value is much faster than under mode II, and that mixed-mode crack growth rates will be somewhere in between [88,90,92]. However, Dillard et al. [93] have shown that in some cases the quasistatic fracture toughness under mode II loading is lower than under mode I loading. Similarly, the critical total energy release rate

($G_T = G_I + G_{II}$) could be lower than the critical rate for either of the pure modes. Dillard et al. explained this behavior by suggesting that shearing could steer the crack to areas that had lower resistance to crack growth. While Dillard et al. investigated quasistatic crack growth, there is a good chance their results will also hold for fatigue crack growth. This suggests that simply basing crack growth calculations on the mode I behavior might not always be conservative for fatigue. Instead, the fatigue crack growth rates should be characterized for a range of mode-mix ratios, or using a geometry that will reproduce the mode-mixity that will be encountered in the intended design (e.g., the CLS configuration).

A very straightforward approach to dealing with mode-mixity is to simply compute the total SERR, G_T, and insert this into an equation with the form of Eq. (19.5). However, in this case the coefficient and exponent will be different for different mode-mix ratios [90,94]. Kenane and Benzeggagh therefore proposed explicitly making both the exponent and coefficient in the Paris equation (Eq. 19.5) functions of the ratio G_{II}/G_T [94]. Instead of varying the Paris parameters, Jones et al. [81,95] propose using Eq. (19.6), but with a value of $\Delta\sqrt{G_{\mathrm{th}}}$ that depends on the mode-mix. An alternative approach has more recently been proposed by Quaresimin et al. [90]. In their approach, which was validated experimentally for a two-part epoxy adhesive, the crack growth rate at mode-mixity values G_{II}/G_T below 0.5 is predicted purely based on the mode I component, with ΔG_I as the controlling parameter. For mode-mixity values above 0.5, the controlling parameter is instead ΔS, where S is the average of the maximum principal stress in a given control volume, which is taken to be representative for the process zone. Prediction of mixed mode crack growth can also be addressed numerically via a cohesive zone model, as for example in the work of Robinson et al. [96], de Moura and Gonçalves [71], Tserpes and Floros [72], Zhang et al. [63], Hosseini-Toudeshky et al. [62], Rocha et al. [70], and Moreira et al. [86]. The precise approach taken differs, but all the mentioned works assume that a cohesive element is fully damaged when exceeding a criterion of the form:

$$\left(\frac{G_I}{G_{Ic}}\right)^{\alpha/2} + \left(\frac{G_{II}}{G_{IIc}}\right)^{\alpha/2} = 1 \tag{19.11}$$

Additionally, a damage parameter is introduced in the constitutive law of the cohesive element, which allows the fatigue-driven damage progression to be modeled, usually by matching the crack growth rate given by some variation of Eq. (19.5).

Most researchers simply take $\alpha = 2$, that is, a linear fracture criterion, but Robinson et al. [96] preferred an elliptical criterion with $2 \leq \alpha \leq 4$. Zhang et al. also use a linear criterion, but introduce a coupling in the traction-separation relations [63]. Rocha et al. [70] instead make use of the Benzeggagh-Kenane criterion [97]. Tserpes and Floros have shown that such a technique (if suitable experimental calibration data are available) can predict not just the crack length, but also for example the twisting of the crack front that occurs in a cracked lap shear specimen based on an epoxy adhesive [72].

19.6.4 Variable amplitude

So far, only a few researchers have attempted to apply fracture mechanics-based models to variable amplitude fatigue. Erpolat et al. [42] applied a numerical integration of Eq. (19.5) to predict the crack length, thereby assuming a linear damage accumulation. However, when compared to experiments on a single part epoxy paste adhesive, they found that the prediction tended to underestimate the crack length, especially after an overload. They attributed this to the model not taking into account that the overload creates a damage zone ahead of the crack tip, which accelerates the crack growth in subsequent cycles. This argument seems reasonable for brittle adhesives, but may not apply to more ductile adhesives. Ashcroft suggested taking the overload effect into account by shifting the constant amplitude fatigue crack growth rate vs the SERR range curve [98]. More recently, Hosseini-Toudeshky et al. [99] and Khoramishad et al. [100] proposed using CZM-based progressive damage models to predict the effect of VA fatigue loading. Khoramishad et al. [100] also presented an experimental validation with data from a toughened epoxy film adhesive, which showed good agreement with the model.

19.7 Effect of joint features

Various geometrical and material features of a joint will affect its fatigue performance The adherend stiffness (i.e., elastic modulus and dimensions) and geometrical shape (e.g., tapered vs constant thickness adherends) will affect the stress distribution in the joint, and thereby also the fatigue life. The overlap length will (beyond a certain minimum length) typically not affect the peak stresses. However, the longer the overlap, the further a crack can grow before the remaining material fails. In this way, the overlap length can still affect the fatigue life of the joint.

The importance of the surface treatment on joint strength has already been discussed, and this is also dependent on failure mode. If the damage mode remains a cohesive failure of the adhesive, the surface treatment does not have a large effect. For example, the study of Azari et al. [101] suggested that as long as the crack propagates within the adhesive sufficiently far from the interface, it is not affected by the surface roughness.

Chapter 18 focuses on the effects of adhesive thickness on various properties. Regarding its effect on crack growth rate specifically, this has been investigated by a number of researchers, including Azari et al. [102,103], Chai [104], Krenk et al. [105], Abou-Hamda et al. [106], Mall and Ramamurthy [107], Xu et al. [108], Schmueser [109], Joseph et al. [110], Wilson [111], and Pascoe et al. [112]. In general, it is reported that an increase in bondline thickness results in a lower crack growth rate (at the same applied SERR), which is attributed to a removal of constraint, allowing more plasticity to occur. However, Krenk et al. [105], Schmueser [109], and Pascoe et al. [112] reported a higher crack growth rate for increasing thickness (all for epoxy adhesives). Pascoe et al. further noted that the energy dissipation per unit of crack growth did not appear to be affected by the adhesive thickness, but that a higher thickness resulted in more energy dissipation per cycle, suggesting more energy was available for crack growth. Chai [104] reported a nonmonotonic behavior for one of the adhesives investigated (PEEK resin). This nonmonotonic behavior was explained by Kinloch and Shaw [113] and Yan et al. [114], who proposed that there is an optimum thickness at which the fracture toughness of the adhesive is maximized. Below this optimum thickness, the plastic zone cannot fully develop while above the optimum thickness, according to Kinloch and Shaw, the plastic zone is less constrained in the thickness direction and therefore does not extend as far ahead of the crack tip. On the other hand, Yan et al. suggested that there is more crack tip blunting, and thus easier void coalescence at higher thicknesses. From the literature, we can thus draw the conclusion that the highest fatigue life can be obtained if the adhesive has the optimum thickness, which can in principle be found by modeling the plastic zone at the crack tip, noting that the plastic zone size is time and temperature dependent.

A step beyond changing the bondline thickness to affect the fatigue life is the inclusion of specific features in the bond to slow or even arrest the growth of cracks. Kruse et al. [115] investigated two options for this: (i) inserting bolts through the adhesive joint, and (ii) using a laser to expose fibers at the surface of a CFRP adherend. The latter approach is used to create through-thickness reinforcement of the adhesive layer. Both approaches appeared to be promising. Chowdhury et al. [116] reported that hybrid joints, combining both fasteners and adhesive, had a higher fatigue life than purely bolted or purely bonded joints. Rather than inserting a bolt through the entire thickness, Löbel et al. [117] and Steinmetz et al. [118] developed a crack stopper based on inserting a different polymer into the bondline. All these strategies of course involve additional manufacturing effort, and thus a careful trade-off is needed at the design stage to decide whether such crack-stopping capability is worth the additional cost. Within the aerospace industry, these approaches are of interest due to the difficulty of certifying adhesive bonds for safety critical structures. Having a proven capability to arrest cracks through a design feature of the bond is seen as a potential strategy for enabling certification [115], as discussed in more detail in Chapter 23.

19.8 Environmental and loading effects

Both the environment and the loading rate can affect the fatigue life. Ramírez et al. [119] recently reviewed the existing literature on the effect of the two most important environmental aspects, temperature and moisture. The review notes that environment and fatigue can have a synergistic effect, where adverse environments (high temperatures and high levels of moisture) cause acceleration of (fatigue) damage accumulation. Ramírez et al. further noted that investigations of environmental effects on fatigue are still largely empirical, and that available models are also still heavily reliant on test data for calibration. A general model for the effect of temperature and moisture on fatigue is still lacking [119].

It is important to note that different adhesives will have a different sensitivity to temperature and moisture. For example, recently Houjou et al. [120] (epoxy), Mu et al. [121] (epoxy), Tan et al. [122] (polyurethane), and Xie et al. [123] (epoxy + sand bonding medium) reported a reduced fatigue life at an increased test temperature. On the other hand, Pugstaller and Wallner [124] saw little difference in the crack growth rates in tests conducted at 23°C and 60°C on a steel laminate bonded with a waterborne epoxy varnish. They suggested this was due to 60°C being far away from the adhesive's glass transition temperature. An even more remarkable result was found by van den Akker et al. [125]. They investigated fatigue-driven disbonding of composite stiffeners bonded with an epoxy film adhesive, aged by exposure to 90% relative humidity at 80°C for 280–396 days and then tested at room temperature. In this case, the disbond growth rate was found to be slower in the aged panels. Van den Akker et al. attributed this to moisture causing plasticization of the adhesive, which resulted in an increased fracture toughness. Taken together, the results discussed above show the importance of understanding the properties of the specific adhesive being used in a particular application. Even which combination of temperature and moisture will result in the worst-case fatigue behavior may differ from adhesive to adhesive.

A final important effect on fatigue of adhesives is the effect of the loading frequency. At high frequencies, self-heating of the adhesive may occur, in which case the elevated temperature can accelerate the fatigue process. In addition, if the temperature reaches or exceeds the glass transition temperature, sudden stiffness changes may occur, resulting in changes of deformations and redistribution of stresses. Many practical applications will not encounter such high frequencies in service. Nevertheless, the self-heating effect limits the highest loading frequencies that can be applied in laboratory tests, forming an obstacle to conducting accelerated fatigue tests.

At the other end of the scale, at very low frequencies, the adhesive will spend long periods of time in the highly loaded portion of the cycle, and thus interactions between creep and fatigue mechanisms can occur. For adhesive bonds, not much work has been published on this topic. Landes and Begley [126], Nikbin et al. [127], and Saxena [128] all developed time-dependent fracture mechanics parameters to take the creep effect into account. Al-Ghamdi [129] proposed four different methods for dealing with combined creep and fatigue. The first method is to fit a purely empirical crack growth law to experimental data. The second method is to assume that creep and fatigue methods are competing, with the growth rate determined by the dominant mechanism. The third method is to partition the crack growth into a component that is time dependent (i.e., creep-driven) and one that is load cycle dependent (i.e., fatigue driven). The fourth method is an extension of the third method, including an empirical term to account for interaction between creep and fatigue mechanisms. A partition method has also been proposed by Movahedi-Rad et al. [130]. In their method, a stress vs time-to-failure curve is predicted based on a combination of the cyclic loading and creep contributions. Each of the individual contributions is scaled based on the energy dissipation in each damage mode. Given that in practical applications adhesive joints may spend a significant portion of their life at high loads, further research into creep-fatigue interactions is called for.

19.9 Damage mechanics

Damage mechanics is an approach to predicting failure in a material by relating the applied load to a deterioration in mechanical properties, which may include stiffness, strength and/or fracture resistance, and resistance to fatigue loading. The aim in damage mechanics is to enable a quantitative representation of load-induced microdamage, such as that commonly observed in areas of high stress concentration prior to the formation of a macrocrack. In an adhesively bonded joint, stress and, hence, any load-induced damage, will tend to be localized. Hence, we may have some areas of the joint undamaged, some areas in various states of damage, and some areas having failed. The net effect of this variation in damage across the joint will always be a net decrease in resistance to further loading compared to the joint prior to loading. A feature of fatigue loading is that the damage across the joint will progressively increase as a function of fatigue cycles until there is sufficient damage to cause complete failure of the joint. An advantage of the damage mechanics approach, compared to other fatigue modeling methods, is that it more closely represents damage evolution as a function of cycling and hence is better placed to determine the residual strength and stiffness at any point in the fatigue life. It can also be used with NDE techniques as part of a health monitoring scheme. The disadvantages of damage mechanics methods are that they tend to be more complex and require more input parameters than alternative fatigue modeling methods.

Two forms of progressive damage modeling that have been used with adhesive joints are cohesive zone modeling (CZM), where the failure is localized along a plane, and continuum damage modeling (CDM), where the damage is in a more extended damage, or process, zone. CZM can be viewed as an extension to the fracture mechanics approach for modeling fatigue behavior, and as such is discussed in the previous section. Hence, this section will be limited to the application of CDM to the prediction of fatigue failure in adhesively bonded joints.

Continuum damage mechanics (CDM) requires a damage variable, D, to be defined as a measure of the severity of the material damage [131–133]. It is assumed that D is equal to 0 for undamaged material and $D = 1$ represents the complete rupture of the material. A simple method of defining D is to relate damage to a reduction in stiffness:

$$D = 1 - \frac{E_D}{E} \tag{19.12}$$

where E and E_D are the Young's modulus of the undamaged and damaged material, respectively. A damage equivalent effective stress, σ^*_{eff}, can be related to damage as:

$$\sigma^*_{\text{eff}} = \frac{\sigma^*}{(1 - D)} \tag{19.13}$$

where σ^* is the damage equivalent stress, which is defined as:

$$\sigma^* = \sigma_{\text{eq}}\left[\frac{2}{3}(1 + \upsilon) + 3(1 - 2\upsilon)\left(\frac{\sigma_H}{\sigma_{\text{eq}}}\right)^2\right]^{\frac{1}{2}} \tag{19.14}$$

where σ_{eq} is the von Mises equivalent stress and σ_H is the hydrostatic stress. σ^*_{eff} can be used as a quasistatic failure criterion. However, to apply the CDM approach to fatigue, Lemaitre [131,132] derived the following equation for the rate of damage accumulation as a function of fatigue cycles, $\delta D/\delta N$:

$$\frac{\delta D}{\delta N} = \frac{2B_0\left[\frac{2}{3}(1+\upsilon) + 3(1-2\upsilon)\left(\frac{\sigma_H}{\sigma_{\text{eq}}}\right)^2\right]^{S_o}}{(\beta_o + 1)(1-D)^{\beta_o+1}}\left(\sigma_{\text{eq, max}}^{\beta_o+1} - \sigma_{\text{eq, min}}^{\beta_o+1}\right) \tag{19.15}$$

where s_o, B_o, and β_o are material- and temperature-dependent coefficients, and $\sigma_{\text{eq, max}}$ and $\sigma_{\text{eq, min}}$ are maximum and minimum von Mises equivalent stresses in a fatigue cycle, respectively. Eq. (19.15) can be integrated for constant amplitude fatigue loading. Using the boundary conditions ($N = 0 \rightarrow D = 0$) and ($N = N_R$ [number of cycles to rupture] $\rightarrow D = 1$):

$$N_R = \frac{(\beta_0 + 1)\left(\sigma_{\text{eq, max}}^{\beta_o+1} - \sigma_{\text{eq, min}}^{\beta_o+1}\right)^{-1}}{2(\beta_o + 2)\beta_o\left[\frac{2}{3}(1+\upsilon) + 3(1-2\upsilon)\left(\frac{\sigma_H}{\sigma_{\text{eq}}}\right)^2\right]^{s_\upsilon}} \tag{19.16}$$

Abdel Wahab et al. [134] used this CDM approach to predict fatigue thresholds in CFRP/epoxy lap-strap joints and double-lap joints. They found that the predictions using CDM compared favorably with those using fracture mechanics. The method was extended to predict fatigue damage in bulk adhesive samples [135] and aluminum/epoxy single-lap joints by Hilmy et al. [136]. A simplified equation for small stress ratio values was also derived, assuming an initial condition of $D = 0$;

$$D = 1 - \left[1 - A(\beta + m + 1)\Delta\sigma_{\text{eq}}{}^{\beta+m} R_v^{\frac{\beta}{2}} N\Big)\right]^{\frac{1}{\beta+m+1}} \tag{19.17}$$

where $\Delta\sigma_{\text{eq}}$ is the von Mises stress range, R_v is the triaxiality function (which is the square of the ratio of the damage equivalent stress to the von Mises equivalent stress), m is the power constant in the Ramberg-Osgood equation, and A and β are experimentally determined damage parameters. The number of cycles to failure (N_f) can be determined from the equation when $D = 1$ and $N = N_f$ at the fully damaged state as:

$$N_f = \frac{\Delta\sigma_{\text{eq}}{}^{-\beta-m} R_v{}^{-\frac{\beta}{2}}}{A\ (\beta + m + 1)} \tag{19.18}$$

A and β are experimentally determined damage parameters. Abdel Wahab et al. [134] used two points from constant amplitude fatigue experiments of CFRP-epoxy double-lap joints to determine these parameters for a particular adhesive at a particular temperature, and showed that Eq. (19.18) could accurately predict a stress life (S-N) curve.

Wahab et al. [137] extended this approach to the low cycle fatigue of bulk adhesive. In this case, the damage evolution curves were derived assuming isotropic damage and a stress triaxiality function equal to one. Application of this method to single-lap joints [138] required determination of the triaxiality function to account for the multiaxial stress state in the joint, and it was seen that this value varied along the adhesive layer. The dependency of the triaxiality function on the joint type was further investigated by Wahab [139,140] in later work.

Although the CDM approach described above enabled the progressive degradation of the adhesive layer to be characterized, it did not allow the initiation and propagation phases of fatigue to be explicitly modeled. Ashcroft et al. [141] used a simple CDM-based approach to progressively model the initiation and evolution of damage in an adhesive joint, leading to crack formation and growth. In this approach, the damage rate dD/dN was assumed to be a power law function of the localized equivalent plastic strain range, $\Delta\varepsilon_p$, that is,

$$\frac{dD}{dN} = C_D\left(\Delta\varepsilon_p\right)^{m_D} \tag{19.19}$$

where C_D and m_D are experimentally derived constants. The rate of damage was determined from FEA using Eq. (19.19) and the element properties were degraded as:

$$\begin{aligned} E &= E_0(1-D) \\ \sigma_{yp} &= \sigma_{yp0}(1-D) \\ \beta &= \beta_0(1-D) \end{aligned} \tag{19.20}$$

where E_0, σ_{yp0}, and β_0 are the Young's modulus, yield stress, and plastic surface modifier constant for the parabolic Mohr-Coulomb model, respectively, and $D=1$ represents a fully damaged element, which was used to define the macrocrack length. E, σ_{yp}, and β are the values of the Young's modulus, yield stress, and plastic surface modifier constant, respectively, after incorporating the material damage. Shenoy et al. [142] showed that this method could be used to predict total-life plots, the fatigue initiation life, fatigue crack growth curves, and strength and stiffness wearout plots; hence, they termed this a unified fatigue methodology (UFM). Shenoy et al. [143] later showed that this approach could also be applied to variable amplitude fatigue.

Walander et al. [144] experimentally studied mode I fatigue crack growth in rubber- and polyurethane-based adhesives using a double-cantilever beam specimen. A damage growth law with a constitutive relation for the adhesive material degradation was implemented in a commercial finite element code. The presented damage evolution law was of the form:

$$\frac{dD}{dN} = \alpha\left(\frac{\frac{\sigma}{1-D} - \sigma_{\text{th}}}{\sigma_{\text{th}}}\right)^{\beta} \tag{19.21}$$

The material parameters: α, β, and σ_{th}, were determined experimentally and good correlation between the experimental data and the proposed damage law for fatigue was reported.

19.10 Summary

This chapter has summarized the current state of the art with regard to evaluating and predicting fatigue of adhesive bonds, which is critical to ensuring their long-term structural integrity. Four broad categories of fatigue models exist, which are stress/strain-life models, strength/stiffness wearout models, damage mechanics, and fracture mechanics. All adhesive fatigue models are still strongly reliant on experimental data for calibration, and an underlying physical theory for predicting the fatigue behavior is still lacking. When generating experimental data, care needs to be taken that the experiments are sufficiently representative of the application of interest, especially ensuring that the same failure mode is observed. Additionally, consideration should be given to stress distributions within the joint (including the proportions of peel and shear stresses) as well as the effects of manufacturing processes, loading frequency, and operational environment.

References

[1] J.Y. Goh, S. Georgiadis, A.C. Orifici, and C.H. Wang, "Effects of bondline flaws on the damage tolerance of composite scarf joints," Compos. Part A Appl. Sci. Manuf., vol. 55, pp. 110–119, 2013.

[2] J. Kupski, S. Teixeira de Freitas, D. Zarouchas, P.P. Camanho, and R. Benedictus, "Composite layup effect on the failure mechanism of single lap bonded joints," Compos. Struct., vol. 217 December 2018, pp. 14–26, 2019.

[3] A. Graner Solana, A.D. Crocombe, and I.A. Ashcroft, "Fatigue life and backface strain predictions in adhesively bonded joints," Int. J. Adhes. Adhes., vol. 30, no. 1, pp. 36–42, 2010.

[4] Z. Zhang, J.K. Shang, and F.V. Lawrence, "A backface strain technique for detecting fatigue crack initiation in adhesive joints," J. Adhes., vol. 49, no. 1–2, pp. 23–36, 1995.

[5] D.R. Lefebvre, B.K. Ahn, D.A. Dillard, and J.G. Dillard, "The effect of surface treatments on interfacial fatigue crack initiation in aluminum/epoxy bonds," Int. J. Fract., vol. 114, no. 2, pp. 191–202, 2002.

[6] M.Z. Sadeghi *et al*., "Damage detection in adhesively bonded single lap joints by using backface strain: proposing a new position for backface strain gauges," Int. J. Adhes. Adhes., vol. 97, 2019, p. 102494, 2020.

[7] D.R. Lefebvre and D.A. Dillard, "A stress singularity approach for the prediction of fatigue crack initiation in adhesive bonds. Part 1: theory," J. Adhes., vol. 70, no. 1–2, pp. 119–138, 1999.

[8] D.R. Lefebvre, D.A. Dillard, and J.G. Dillard, "A stress singularity approach for the prediction of fatigue crack initiation in adhesive bonds. Part 2: experimental," J. Adhes., vol. 70, no. 1–2, pp. 139–154, 1999.

[9] G. Zambelis, T. Da Silva Botelho, O. Klinkova, I. Tawfiq, and C. Lanouette, "Evaluation of the energy release rate in mode I of asymmetrical bonded composite/metal assembly," Eng. Fract. Mech., vol. 190, pp. 175–185, 2018.

[10] G. Zambelis, T. Da Silva Botelho, O. Klinkova, I. Tawfiq, and C. Lanouette, "A new approach in testing fatigue fracture mechanics properties in asymmetrical bonded composite/metal assemblies," Compos. Part B Eng., vol. 158, 2018, pp. 390–399, 2019.

[11] L. Adamos and T. Loutas, "Challenges in the fatigue crack growth characterization of metal/composite joints: a compliance-based investigation of a Ti/CFRP joint," Int. J. Fatigue, vol. 148, p. 106233, 2021.
[12] W.D. Hartley *et al*., "Fracture characterization of overmold composite adhesion," J. Thermoplast. Compos. Mater., vol. 35, no. 7, pp. 977–997, 2022.
[13] Y.H. Lai, M.D. Rakestraw, and D.A. Dillard, "The cracked lap shear specimen revisited—a closed form solution," Int. J. Solids Struct., vol. 33, no. 12, pp. 1725–1743, 1996.
[14] M.K. Budzik *et al*., "Testing mechanical performance of adhesively bonded composite joints in engineering applications: an overview," J. Adhes., 2021.
[15] J.A. Pascoe, C.D. Rans, and R. Benedictus, "Characterizing fatigue delamination growth behaviour using specimens with multiple delaminations: the effect of unequal delamination lengths," Eng. Fract. Mech., vol. 109, pp. 150–160, 2013.
[16] R. Sahin and S. Akpinar, "The effects of adherend thickness on the fatigue strength of adhesively bonded single-lap joints," Int. J. Adhes. Adhes., vol. 107, p. 102845, 2021.
[17] A.I.M. Foletti, J. Sena Cruz, and A.P. Vassilopoulos, "Fabrication and curing conditions effects on the fatigue behavior of a structural adhesive," Int. J. Fatigue, vol. 139, p. 105743, 2020.
[18] W. Seneviratne, J. Tomblin, and M. Kittur, "Durability and residual strength of adhesively-bonded composite joints: the case of F/A-18 A-D wing root stepped-lap joint," in Fatigue and Fracture of Adhesively-Bonded Composite Joints, A.P. Vassilopoulos, Ed. Cambridge: Elsevier, 2015, pp. 289–320.
[19] E.M. Mueller, S. Starnes, N. Strickland, P. Kenny, and C. Williams, "The detection, inspection, and failure analysis of a composite wing skin defect on a tactical aircraft," Compos. Struct., vol. 145, pp. 186–193, 2016.
[20] A. Wöhler, "Versuche über die Festigkeit der Eisenbahnwagenachsen," Zeitschrift für Bauwes., vol. 10, 1867.
[21] A.J. Kinloch and S.O. Osiyemi, "Predicting the fatigue life of adhesively-bonded joints," J. Adhes., vol. 43, no. 1–2, pp. 79–90, 1993.
[22] M.M. Abdel Wahab, I.A. Ashcroft, A.D. Crocombe, and P.A. Smith, "Numerical prediction of fatigue crack propagation lifetime in adhesively bonded structures," Int. J. Fatigue, vol. 24, no. 6, pp. 705–709, 2002.
[23] J.A. Harris and P.A. Fay, "Fatigue life evaluation of structural adhesives for automative applications," Int. J. Adhes. Adhes., vol. 12, no. 1, pp. 9–18, 1992.
[24] A.D. Crocombe, C.Y. Ong, C.M. Chan, M.M. Abdel Wahab, and I.A. Ashcroft, "Investigating fatigue damage evolution in adhesively bonded structures using backface strain measurement," J. Adhes., vol. 78, no. 9, pp. 745–776, 2002.
[25] A.G. Solana, A.D. Crocombe, M.M.A. Wahab, and I.A. Ashcroft, "Fatigue initiation in adhesively-bonded single-lap joints," J. Adhes. Sci. Technol., vol. 21, no. 14, pp. 1343–1357, 2007.
[26] V. Shenoy, I.A. Ashcroft, G.W. Critchlow, A.D. Crocombe, and M.M. Abdel Wahab, "An investigation into the crack initiation and propagation behaviour of bonded single-lap joints using backface strain," Int. J. Adhes. Adhes., vol. 29, no. 4, pp. 361–371, 2009.
[27] M. Dessureautt and J.K. Spelt, "Observations of fatigue crack initiation and propagation in an epoxy adhesive," Int. J. Adhes. Adhes., vol. 17, no. 3, pp. 183–195, 1997.
[28] M. Quaresimin and M. Ricotta, "Fatigue behaviour and damage evolution of single lap bonded joints in composite material," Compos. Sci. Technol., vol. 66, no. 2, pp. 176–187, 2006.
[29] A. Palmgren, "Die lebensdauer von kugellargen," Z. Ver. Dtsch. Zucker Ind., vol. 68, pp. 339–41, 1924.

[30] M.A. Miner, “Cumulative damage in fatigue,” J. Appl. Mech., vol. 12, pp. 159–64, 1945.
[31] S.M. Marco and W.L. Starkey, “A concept of fatigue damage,” Trans. Am. Soc. Mech. Eng., vol. 76, pp. 626–662, 1954.
[32] D.L. Henry, “A theory of fatigue damage accumulation in steel,” Trans. Am. Soc. Mech. Eng., vol. 9, no. 13, p. 918, 1955.
[33] H.L. Leve, “Cumulative damage theories,” in Metal Fatigue: Theory and Design, NY, USA: John Wiley & Sons, 1969, pp. 170–203.
[34] M.J. Owen and R.J. Howe, “The accumulation of damage in a glass-reinforced plastic under tensile and fatigue loading,” J. Phys. D. Appl. Phys., vol. 5, no. 9, pp. 1637–1649, 1972.
[35] I.P. Bond, “Fatigue life prediction for GRP subjected to variable amplitude loading,” Compos. Part A Appl. Sci. Manuf., vol. 30, no. 8, pp. 961–970, 1999.
[36] S. Erpolat, I.A. Ashcroft, A.D. Crocombe, and M.M. Abdel-Wahab, “A study of adhesively bonded joints subjected to constant and variable amplitude fatigue,” Int. J. Fatigue, vol. 26, no. 11, pp. 1189–1196, 2004.
[37] M.M.A. Wahab, I.A. Ashcroft, A.D. Crocombe, D.J. Hughes, and S.J. Shaw, “Effect of environment on the fatigue of bonded composite joints. Part 2: fatigue threshold prediction,” Compos. Part A Appl. Sci. Manuf., vol. 32, no. 1, pp. 59–69, 2001.
[38] V. Shenoy, I.A. Ashcroft, G.W. Critchlow, A.D. Crocombe, and M.M. Abdel Wahab, “Strength wearout of adhesively bonded joints under constant amplitude fatigue,” Int. J. Fatigue, vol. 31, no. 5, pp. 820–830, 2009.
[39] V. Shenoy, I.A. Ashcroft, G.W. Critchlow, A.D. Crocombe, and M.M. Abdel Wahab, “An evaluation of strength wearout models for the lifetime prediction of adhesive joints subjected to variable amplitude fatigue,” Int. J. Adhes. Adhes., vol. 29, no. 6, pp. 639–649, 2009.
[40] J.R. Schaff and B.D. Davidson, “Life prediction methodology for composite structures. Part I—constant amplitude and two-stress level fatigue,” J. Compos. Mater., vol. 31, no. 2, pp. 128–157, 1997.
[41] J.R. Schaff and B.D. Davidson, “Life prediction methodology for composite structures. Part II—spectrum fatigue,” J. Compos. Mater., vol. 31, no. 2, pp. 158–181, 1997.
[42] S. Erpolat, I.A. Ashcroft, A.D. Crocombe, and M.M. Abdel-Wahab, “Fatigue crack growth acceleration due to intermittent overstressing in adhesively bonded CFRP joints,” Compos. Part A Appl. Sci. Manuf., vol. 35, no. 10, pp. 1175–1183, 2004.
[43] D.M. Neto, E.R. Sérgio, M.F. Borges, L.P. Borrego, and F.V. Antunes, “Effect of load blocks on fatigue crack growth,” Int. J. Fatigue, vol. 162, p. 107001, 2022.
[44] A.T. Dibenedetto and G. Salee, “Fatigue crack propagation in, graphite fiber reinforced nylon 66,” Polym. Eng. Sci., vol. 19, no. 7, pp. 512–518, 1979.
[45] J.N. Yang, D.L. Jones, S.H. Yang, and A. Meskini, “A stiffness degradation model for graphite/epoxy laminates,” J. Compos. Mater., pp. 753–769, 1990.
[46] H.A. Whitworth, “Cumulative damage in composites,” J. Eng. Mater. Technol., vol. 112, no. 3, pp. 358–361, 1990.
[47] Y. Liu, X. Zhang, S. Lemanski, H.Y. Nezhad, and D. Ayre, “Experimental and numerical study of process-induced defects and their effect on fatigue debonding in composite joints,” Int. J. Fatigue, vol. 125, 2018, pp. 47–57, 2019.
[48] P.C. Paris, M.P. Gomez, and W.E. Anderson, “A rational analytic theory of fatigue,” Trend Eng., vol. 13, pp. 9–14, 1961.
[49] S. Mostovoy and E.J. Ripling, “Flaw tolerance of a number of commercial and experimental adhesives,” in Adhesion Science and Technology, no. 9B, L.-H. Lee, Ed. New York: Plenum Press, 1975, pp. 513–562.

[50] C. Rans, R.C. Alderliesten, and R. Benedictus, "Misinterpreting the results: how similitude can improve our understanding of fatigue delamination growth," Compos. Sci. Technol., vol. 71, pp. 230–238, 2011.
[51] J.A. Pascoe, R.C. Alderliesten, and R. Benedictus, "Methods for the prediction of fatigue delamination growth in composites and adhesive bonds—a critical review," Eng. Fract. Mech., vol. 112–113, pp. 72–96, 2013.
[52] I.A. Ashcroft and A. Mubashar, "Fatigue," in Adhesive Bonding—Science, Technology and Applications, second ed., R.D. Adams, Ed. Duxford: Woodhead Publishing, 2021, pp. 317–361.
[53] M.M. Abdel Wahab, "Fatigue in adhesively bonded joints: a review," ISRN Mater. Sci., vol. 2012, no. c, pp. 1–25, 2012.
[54] P. Gaur and R.S. Prasad, "Investigation of fatigue crack propagation in adhesively bonded joints using fatigue testing, finite element analysis and neural networks," Appl. Eng. Lett., vol. 4, no. 4, pp. 136–149, 2019.
[55] Q. Chen, H. Guo, K. Avery, X. Su, and H. Kang, "Fatigue performance and life estimation of automotive adhesive joints using a fracture mechanics approach," Eng. Fract. Mech., vol. 172, pp. 73–89, 2017.
[56] W.J. Lai and J. Pan, "Stress intensity factor solutions for adhesive-bonded lap-shear specimens of magnesium and steel sheets with and without kinked cracks for fatigue life estimations," Eng. Fract. Mech., vol. 131, pp. 454–470, 2014.
[57] E.F. Rybicki and M.F. Kanninen, "A finite element calculation of stress intensity factors by a modified crack closure integral," Eng. Fract. Mech., vol. 9, no. 4, pp. 931–938, 1977.
[58] G.R. Irwin, "Analysis of stresses and strains near the end of a crack traversing a plate," J. Appl. Mech., vol. 24, no. 3, pp. 361–364, 1957.
[59] R. Krueger, "Virtual crack closure technique: history, approach, and applications," Appl. Mech. Rev., vol. 57, no. 1–6, pp. 109–143, 2004.
[60] L.R. Deobald *et al*., "Guidelines for VCCT-Based Interlaminar Fatigue and Progressive Failure Finite Element Analysis," NASA/TM–2017-219663, 2017.
[61] M.F.S.F. De Moura and J.P.M. Gonçalves, "Cohesive zone model for high-cycle fatigue of adhesively bonded joints under mode i loading," Int. J. Solids Struct., vol. 51, no. 5, pp. 1123–1131, 2014.
[62] H. Hosseini-Toudeshky, F. Sheibanian, H.R. Ovesy, and M.S. Goodarzi, "Prediction of interlaminar fatigue damages in adhesively bonded joints using mixed-mode strain based cohesive zone modeling," Theor. Appl. Fract. Mech., vol. 106, p. 102480, 2020.
[63] W. Zhang, Z. Tang, Y. Yang, J. Wei, and P. Stanislav, "Mixed-mode debonding behavior between CFRP plates and concrete under fatigue loading," J. Struct. Eng., vol. 147 (5), p. 04021055, 2021.
[64] K. Tserpes *et al*., "A review on failure theories and simulation models for adhesive joints," J. Adhes., pp. 1–61, 2021.
[65] R.D.F. Moreira, M.F.S.F. de Moura, F.G.A. Silva, F.M.G. Ramírez, and F.D.R. Silva, "Numerical comparison of several composite bonded repairs under fatigue loading," Compos. Struct., vol. 243, p. 112250, 2020.
[66] A. Pirondi and F. Moroni, "Improvement of a cohesive zone model for fatigue delamination rate simulation," Materials (Basel)., vol. 12, no. 1, pp. 1–17, 2019.
[67] A. Pirondi, G. Giuliese, and F. Moroni, "Fatigue debonding three-dimensional simulation with cohesive zone," J. Adhes., vol. 92, no. 7–9, pp. 553–571, 2016.
[68] A. Pirondi, G. Giuliese, F. Moroni, A. Bernasconi, and A. Jamil, "Comparative study of cohesive zone and virtual crack closure techniques for three-dimensional fatigue debonding," J. Adhes., vol. 90, no. 5–6, pp. 457–481, 2014.

[69] A. Pirondi and F. Moroni, "Simulation of mixed-mode I/II fatigue crack propagation in adhesive joints with a modified cohesive zone model," J. Adhes. Sci. Technol., vol. 25, no. 18, pp. 2483–2499, 2011.

[70] A.V.M. Rocha *et al.*, "Numerical analysis of mixed-mode fatigue crack growth of adhesive joints using CZM," Theor. Appl. Fract. Mech., vol. 106, 2019, p. 102493, 2020.

[71] M.F.S.F. de Moura and J.P.M. Gonçalves, "Cohesive zone model for high-cycle fatigue of composite bonded joints under mixed-mode I+II loading," Eng. Fract. Mech., vol. 140, pp. 31–42, 2015.

[72] K. Tserpes and I. Floros, "Fatigue crack growth simulation in adhesively bonded composite joints," Fatigue Fract. Eng. Mater. Struct., vol. 42, no. 7, pp. 1430–1440, 2019.

[73] D.S. Dugdale, "Yielding of steel sheets containing slits," J. Mech. Phys. Solids, vol. 8, no. 2, pp. 100–104, 1960.

[74] G.I. Barenblatt, "The mathematical theory of equilibrium cracks in brittle fracture," in Advances in Applied Mechanics, 1962, vol. 7, pp. 55–129.

[75] A. Pirondi and F. Moroni, "A progressive damage model for the prediction of fatigue crack growth in bonded joints," J. Adhes., vol. 86, no. 5–6, pp. 501–521, 2010.

[76] F. Moroni and A. Pirondi, "A procedure for the simulation of fatigue crack growth in adhesively bonded joints based on the cohesive zone model and different mixed-mode propagation criteria," Eng. Fract. Mech., vol. 78, no. 8, pp. 1808–1816, 2011.

[77] J.A. Pascoe, R.C. Alderliesten, and R. Benedictus, "On the physical interpretation of the R-ratio effect and the LEFM parameters used for fatigue crack growth in adhesive bonds," Int. J. Fatigue, vol. 97, pp. 162–176, 2017.

[78] R. Jones, A.J. Kinloch, and W. Hu, "Cyclic-fatigue crack growth in composite and adhesively-bonded structures: the FAA slow crack growth approach to certification and the problem of similitude," Int. J. Fatigue, vol. 88, pp. 10–18, 2016.

[79] J. Andersons, M. Hojo, and S. Ochiai, "Empirical model for stress ratio effect on fatigue delamination growth rate in composite laminates," Int. J. Fatigue, vol. 26, no. 6, pp. 597–604, 2004.

[80] J. Jia and J.F. Davalos, "Study of load ratio for mode-I fatigue fracture of wood-FRP-bonded interfaces," J. Compos. Mater., vol. 38, no. 14, pp. 1211–1230, 2004.

[81] R. Jones, W. Hu, and A.J. Kinloch, "A convenient way to represent fatigue crack growth in structural adhesives," Fatigue Fract. Eng. Mater. Struct., vol. 38, no. 4, pp. 379–391, 2015.

[82] R. Jones, A.J. Kinloch, J. Michopoulos, and A.P. Iliopoulos, "Crack growth in adhesives: similitude and the Hartman-Schijve equation," Compos. Struct., vol. 273, p. 114260, 2021.

[83] R. Khan, "Delamination Growth in Composites Under Fatigue Loading," Delft University of Technology, 2013.

[84] D.R. Atodaria, S.K. Putatunda, and P.K. Mallick, "Delamination growth behavior of a fabric reinforced laminated composite under mode {I} fatigue," J. Eng. Mater. Technol., vol. 121, no. 3, pp. 381–385, 1999.

[85] G. Allegri, M.I. Jones, M.R. Wisnom, and S.R. Hallett, "A new semi-empirical model for stress ratio effect on mode II fatigue delamination growth," Compos. Part A Appl. Sci. Manuf., vol. 42, no. 7, pp. 733–740, 2011.

[86] R.D.F. Moreira, M.F.S.F. de Moura, F.G.A. Silva, J.P.A. Reina, and T.M.S. Rodrigues, "A simple strategy to perform mixed-mode I+II fatigue/fracture characterisation of composite bonded joints," Int. J. Fatigue, vol. 158, 2021, p. 106723, 2022.

[87] F. Castro Sousa, A. Akhavan-Safar, G. Rakesh, and L.F.M. da Silva, "Fatigue life estimation of adhesive joints at different mode mixities," J. Adhes., vol. 98, no. 1, pp. 1–23, 2022.

[88] J. Monteiro *et al.*, "Influence of mode mixity and loading conditions on the fatigue crack growth behaviour of an epoxy adhesive," Fatigue Fract. Eng. Mater. Struct., vol. 43, no. 2, pp. 308–316, 2020.

[89] F.C. Sousa, A. Akhavan-Safar, R. Goyal, and L.F.M. da Silva, "The influence of mode mixity and adhesive system on the fatigue life of adhesive joints," Fatigue Fract. Eng. Mater. Struct., vol. 43, no. 10, pp. 2337–2348, 2020.

[90] M. Quaresimin, P.A. Carraro, G. Meneghetti, and M. Ricotta, Mixed-Mode Fatigue of Bonded Joints in Composites: Experiments and Modelling, no. 2011. Elsevier, 2015.

[91] M. Shahverdi, A.P. Vassilopoulos, and T. Keller, "Mixed-mode fatigue failure criteria for adhesively-bonded pultruded GFRP joints," Compos. Part A Appl. Sci. Manuf., vol. 54, pp. 46–55, 2013.

[92] D. Bürger, "Mixed-Mode Fatigue Disbond on Metallic Bonded Joints," Delft University of Technology, 2015.

[93] D.A. Dillard, H.K. Singh, D.J. Pohlit, and J.M. Starbuck, "Observations of decreased fracture toughness for mixed mode fracture testing of adhesively bonded joints," J. Adhes. Sci. Technol., vol. 23, no. 10–11, pp. 1515–1530, 2009.

[94] M. Kenane and M.L. Benzeggagh, "Mixed-mode delamination fracture toughness of unidirectional glass/epoxy composites under fatigue loading," Compos. Sci. Technol., vol. 57, no. 5, pp. 597–605, 1997.

[95] R. Jones, S. Stelzer, and A.J. Brunner, "Mode I, II and mixed mode I/II delamination growth in composites," Compos. Struct., vol. 110, no. 1, pp. 317–324, 2014.

[96] P. Robinson, U. Galvanetto, D. Tumino, G. Bellucci, and D. Violeau, "Numerical simulation of fatigue-driven delamination using interface elements," Int. J. Numer. Methods Eng., vol. 63, no. 13, pp. 1824–1848, 2005.

[97] M.L. Benzeggagh and M. Kenane, "Measurement of mixed-mode delamination fracture toughness of unidirectional glass/epoxy composites with mixed-mode bending apparatus," Compos. Sci. Technol., vol. 56, no. 4, pp. 439–449, 1996.

[98] I.A. Ashcroft, "A simple model to predict crack growth in bonded joints and laminates under variable-amplitude fatigue," J. Strain Anal. Eng. Des., vol. 39, no. 6, pp. 707–716, 2004.

[99] H. Hosseini-Toudeshky, M. Jahanmardi, and M.S. Goodarzi, "Progressive debonding analysis of composite blade root joint of wind turbines under fatigue loading," Compos. Struct., vol. 120, pp. 417–427, 2015.

[100] H. Khoramishad, A.D. Crocombe, K.B. Katnam, and I.A. Ashcroft, "Fatigue damage modelling of adhesively bonded joints under variable amplitude loading using a cohesive zone model," Eng. Fract. Mech., vol. 78, no. 18, pp. 3212–3225, 2011.

[101] S. Azari, M. Papini, and J.K. Spelt, "Effect of surface roughness on the performance of adhesive joints under static and cyclic loading," J. Adhes., vol. 86, no. 7, pp. 742–764, 2010.

[102] S. Azari, M. Papini, and J.K. Spelt, "Effect of adhesive thickness on fatigue and fracture of toughened epoxy joints—part I: experiments," Eng. Fract. Mech., vol. 78, no. 1, pp. 153–162, 2011.

[103] S. Azari, M. Papini, and J.K. Spelt, "Effect of adhesive thickness on fatigue and fracture of toughened epoxy joints—part II: analysis and finite element modeling," Eng. Fract. Mech., vol. 78, no. 1, pp. 138–152, 2011.

[104] H. Chai, "On the correlation between the mode I failure of adhesive joints and laminated composites," Eng. Fract. Mech., vol. 24, no. 3, pp. 413–431, 1986.

[105] S. Krenk, J. Jönsson, and L.P. Hansen, "Fatigue analysis and testing of adhesive joints," Eng. Fract. Mech., vol. 53, no. 6, pp. 859–872, 1996.

[106] M.M. Abou-Hamda, M.M. Megahed, and M.M.I. Hammouda, "Fatigue crack growth in double cantilever beam specimen with an adhesive layer," Eng. Fract. Mech., vol. 60, no. 5–6, pp. 605–614, 1998.

[107] S. Mall and G. Ramamurthy, "Effect of bond thickness on fracture and fatigue strength of adhesively bonded composite joints," Int. J. Adhes. Adhes., vol. 9, no. 1, pp. 33–37, 1989.
[108] X.X. Xu, A.D. Crocombe, and P.A. Smith, "Fatigue crack growth rates in adhesive joints tested at different frequencies," J. Adhes., vol. 58, no. 3–4, pp. 191–204, 1996.
[109] D.W. Schmueser, "A fracture mechanics approach to characterizing cyclic debonding of varied thickness adhesive joints to electroprimed steel surfaces," J. Adhes., vol. 36, no. 1, pp. 1–23, 1991.
[110] R. Joseph, J.P. Bell, A.J. Mcevily, and J.L. Liang, "Fatigue crack growth in epoxy/aluminum and epoxy/steel joints," J. Adhes., vol. 41, no. 1–4, pp. 169–187, 1993.
[111] G.S. Wilson, "Fatigue Crack Growth Prediction for Generalized Fiber Metal Laminates and Hybrid Materials," Delft University of Technology, 2013.
[112] J.A. Pascoe, N. Zavatta, E. Troiani, and R.C. Alderliesten, "The effect of bond-line thickness on fatigue crack growth rate in adhesively bonded joints," Eng. Fract. Mech., vol. 229, p. 106959, 2020.
[113] A.J. Kinloch and S.J. Shaw, "The fracture resistance of a toughened epoxy adhesive," J. Adhes., vol. 12, no. 1, pp. 59–77, 1981.
[114] C. Yan, Y.W. Mai, and L. Ye, "Effect of bond thickness on fracture behaviour in adhesive joints," J. Adhes., vol. 75, no. 1, pp. 27–44, 2001.
[115] T. Kruse, T. Körwien, S. Heckner, and M. Geistbeck, "Bonding of CFRP primary aerospace structures—crackstopping in composite bonded joints under fatigue," in 20th International Conferences on Composite Materials, 2015.
[116] N.M. Chowdhury, J. Wang, W.K. Chiu, and P. Chang, "Static and fatigue testing bolted, bonded and hybrid step lap joints of thick carbon fibre/epoxy laminates used on aircraft structures," Compos. Struct., vol. 142, pp. 96–106, 2016.
[117] T. Löbel, D. Holzhüter, M. Sinapius, and C. Hühne, "A hybrid bondline concept for bonded composite joints," Int. J. Adhes. Adhes., vol. 68, pp. 229–238, 2016.
[118] J. Steinmetz *et al*., "The working principles of a multifunctional bondline with disbond stopping and health monitoring features for composite structures," J. Compos. Sci., vol. 5, no. 2, pp. 1–17, 2021.
[119] F.M.G. Ramírez, M.F.S.F. de Moura, R.D.F. Moreira, and F.G.A. Silva, "A review on the environmental degradation effects on fatigue behaviour of adhesively bonded joints," Fatigue Fract. Eng. Mater. Struct., vol. 43, no. 7, pp. 1307–1326, 2020.
[120] K. Houjou, K. Shimamoto, H. Akiyama, and C. Sato, "Effect of test temperature on the shear and fatigue strengths of epoxy adhesive joints," J. Adhes., 2021.
[121] W.L. Mu, Q.H. Xu, J.X. Na, H. Wang, W. Tan, and D.F. Li, "Influence of temperature and humidity on the fatigue behaviour of adhesively bonded CFRP/aluminium alloy joints," J. Adhes., 2021.
[122] W. Tan, N. Jingxin, W. Guangbin, H. Chen, and H. Meng, "Effect of temperature on the fatigue performance and failure mechanism of a flexible adhesive butt joint," J. Adhes., 2021.
[123] G. hua Xie, Z.a. Tao, Y. Sun, S.q. Li, and A.A. Gedi, "An investigation of hygrothermal effect on fatigue behavior of adhesively bonded anchorages for FRP tendon," Constr. Build. Mater., vol. 316, 2020, p. 126044, 2022.
[124] R. Pugstaller and G.M. Wallner, "Development of a fracture-mechanics based fatigue testing method for epoxy/electrical steel laminates with thin adhesive layer," Eng. Fract. Mech., vol. 258, p. 108045, 2021.
[125] B.P.H. van den Akker, M.V. Donadon, R. Loendersloot, L.A. de Oliveira, and M.A. Arbelo, "The influence of hygrothermal aging on the fatigue behavior and residual

strength of post-buckled co-bonded stiffened panels subjected to compressive loading," Compos. Part B Eng., vol. 194, , p. 108023, 2020.
[126] J.D. Landes and J.A. Begley, "A fracture mechanics approach to creep crack growth," in Mechanics of Crack Growth, ASTM STP 590, American Society for Testing and Materials, 1976, pp. 128–148.
[127] K.M. Nikbin, G.A. Webster, and C.E. Turner, "Relevance of nonlinear fracture mechanics to creep crack growth," in Crack and Fracture, ASTM STP 601, American Society for Testing and Materials, 1976, pp. 47–62.
[128] A. Saxena, "Creep crack growth under non-steady-state conditions," in Fracture Mechanics, ASTM STP 905, American Society for Testing and Materials, 1986, pp. 185–201.
[129] A.H. Al-Ghamdi, "Fatigue and Creep of Adhesively Bonded Joints," Loughborough University, 2004.
[130] A.V. Movahedi-Rad, G. Eslami, and T. Keller, "A novel fatigue life prediction methodology based on energy dissipation in viscoelastic materials," Int. J. Fatigue, vol. 152, 2021, p. 106457, April.
[131] J. Lemaitre, "How to use damage mechanics," Nucl. Eng. Des., vol. 80, no. 2, pp. 233–245, 1984.
[132] J. Lemaitre, "A continuous damage mechanics model for ductile fracture," J. Eng. Mater. Technol., vol. 107, no. 1, pp. 83–89, January 1985.
[133] L. Kachanov, Introduction to Continuum Damage Mechanics. Dordrecht: Martinus Nijhoff, 1986.
[134] M.M. Abdel Wahab, I.A. Ashcroft, A.D. Crocombe, and S.J. Shaw, "Prediction of fatigue thresholds in adhesively bonded joints using damage mechanics and fracture mechanics," J. Adhes. Sci. Technol., vol. 15, no. 7, pp. 763–781, 2001.
[135] I. Hilmy, M.M. Abdel Wahab, I.A. Ashcroft, and A.D. Crocombe, "Measuring of damage parameters in adhesive bonding," Key Eng. Mater., vol. 324–325, no. 1, pp. 275–278, 2006.
[136] I. Hilmy, M.M. Abdel Wahab, A.D. Crocombe, I.A. Ashcroft, and A.G. Solana, "Effect of triaxiality on damage parameters in adhesive," Key Eng. Mater., vol. 348–349, no. 2, pp. 37–40, 2007.
[137] M.M.A. Wahab, I. Hilmy, I.A. Ashcroft, and A.D. Crocombe, "Evaluation of fatigue damage in adhesive bonding: part 1: bulk adhesive," J. Adhes. Sci. Technol., vol. 24, no. 2, pp. 305–324, 2010.
[138] M.M.A. Wahab, I. Hilmy, I.A. Ashcroft, and A.D. Crocombe, "Evaluation of fatigue damage in adhesive bonding: part 2: single lap joint," J. Adhes. Sci. Technol., vol. 24, no. 2, pp. 325–345, 2010.
[139] M.M.A. Wahab, I. Hilmy, I.A. Ashcroft, and A.D. Crocombe, "Damage parameters of adhesive joints with general triaxiality part I: finite element analysis," J. Adhes. Sci. Technol., vol. 25, no. 9, pp. 903–923, 2011.
[140] M.M.A. Wahab, I. Hilmy, I.A. Ashcroft, and A.D. Crocombe, "Damage parameters of adhesive joints with general triaxiality, part 2: scarf joint analysis," J. Adhes. Sci. Technol., vol. 25, no. 9, pp. 925–947, 2011.
[141] I.A. Ashcroft, V. Shenoy, G.W. Critchlow, and A.D. Crocombe, "A comparison of the prediction of fatigue damage and crack growth in adhesively bonded joints using fracture mechanics and damage mechanics progressive damage methods," J. Adhes., vol. 86, no. 12, pp. 1203–1230, 2010.
[142] V. Shenoy, I.A. Ashcroft, G.W. Critchlow, and A.D. Crocombe, "Unified methodology for the prediction of the fatigue behaviour of adhesively bonded joints," Int. J. Fatigue, vol. 32, no. 8, pp. 1278–1288, 2010.

[143] V. Shenoy, I.A. Ashcroft, G.W. Critchlow, and A.D. Crocombe, "Fracture mechanics and damage mechanics based fatigue lifetime prediction of adhesively bonded joints subjected to variable amplitude fatigue," Eng. Fract. Mech., vol. 77, no. 7, pp. 1073–1090, 2010.
[144] T. Walander, A. Eklind, T. Carlberger, and U. Stigh, "Fatigue damage of adhesive layers—experiments and models," Procedia Mater. Sci., vol. 3, pp. 829–834, 2014.